Journal of Thermal Analysis and Calorimetry, Vol. 70 (2002) 985–994

TA ON Mo(W)/Cu(Ag)/S CLUSTERS DERIVED WITH $[C_p^*MS_3]^-$
Kinetics of $[PPh_4]_2[C_p^*WS_3(CuBr)_3]_2$ and $[PPh_4]_2[C_p^*MoS_3(CuBr)_3]_2$

Z. Lu[1*], *Y. Ding*[1], *Y. Xu*[1], *Z. Yao*[1], *Q. Liu*[2] *and J. Lang*[2]

[1]The Testing and Analysis Center, Suzhou University, Suzhou, Jiangsu 215006, P.R. China
[2]Departments of Chemistry and Chemical Engineering, Suzhou University, Suzhou, Jiangsu 215006,
P.R. China

(Received February 6, 2002; in revised form April 6, 2002)

Abstract

Thermal analysis on two new heterometallic sulfide clusters, $[PPh_4]_2[C_p^*WS_3(CuBr)_3]_2$ and $[PPh_4]_2[C_p^*MoS_3(CuBr)_3]_2$ (where *PPh*$_4$=tetraphenyl phosphonium, C_p^*=pentamethylcyclopentadienyl), was carried out using a simultaneous TG-DTA unit in an atmosphere of flowing nitrogen and at various heating rates. Supplemented using EDS method, their thermal behavior and properties, together with the composition of their intermediate product, were examined and discussed in connection with their distinctive molecular structure as a dianion, which provided some theoretically and practically significant information. Both clusters decomposed in a two-step mode, but without a stable new phase composed of Mo/W–Cu–S formed during their decomposition process as we expected. Based on TG-DTG data, four methods, i.e. Achar–Brindley–Sharp, Coats–Redfern, Kissinger and Flynn–Wall–Ozawa equation, were used to calculate the non-isothermal kinetic parameters and to determine the most probable mechanisms.

Keywords: $[C_p^*MS_3]^-$, Mo/Cu/S cluster, non-isothermal kinetics, thermal decomposition, W/Cu/S cluster

Introduction

Since 1970 sulfur-containing metallic clusters derived with $[MX_4]^{z-}$ (where *M*=Mo, W, V, Re, Nb, Ta; *X*=S, Se; *z*=1–3) have attracted considerable attention [1–3] due to their practical importance in various fields. They can be used for catalytic hydrodesulfurization in petrochemical industry [4], for nitrogen fixation in biomimetic chemistry [5] and as superconducting material [6]. Among them, Mo(W)/Cu(Ag)/S clusters derived with $[C_p^*MS_3]^-$ (where C_p^*=pentamethyl-cyclopentadienyl, *M*=Mo, W) [7] is a new

* Author for correspondence: E-mail: zrlu@suda.edu.cn

1418–2874/2002/ $ 5.00

Akadémiai Kiadó, Budapest
Kluwer Academic Publishers, Dordrecht

member of organometallic family and have been the subject of recent interest owing not only to their distinctive molecular structure as heterometallic sulfide clusters, but also to the fact that they have shown potential as materials for special purposes, such as third-order non-linear optical material [8]. So far as we know, however, there has been little information concerning their thermal properties which is actually quite important for them to be better processed and thus more extensively used.

We [9, 10] have recently reported the preparation and crystal structure of a new sort of clusters, i.e., title compounds $[PPh_4]_2[C_p^*WS_3(CuBr)_3]_2$ and $[PPh_4]_2[C_p^*MoS_3(CuBr)_3]_2$ (where PPh_4=tetraphenyl phosphonium). In order to further investigate their properties and application, we have studied them using TG-DTG-DTA technique. The main objective of this work is to study their thermal stability, thermal behavior and decomposition kinetics. In addition, we wish to find out a proper temperature at which these clusters may be made into thin film by chemical vacuum deposition (CVD) method so that their optical property could be further determined. We also expect to reveal whether some new phases composed of Mo/W–Cu–S exist after their organic group is expelled and whether new phases, if exist, have special properties such as superconductivity.

Experimental

Material

Both dark red crystal of $[PPh_4]_2[C_p^*WS_3(CuBr)_3]_2$ and black crystal of $[PPh_4]_2[C_p^*MoS_3(CuBr)_3]_2$ were freshly prepared following the procedures described in our previous work [9, 10]. The quality of samples for TA study in the present work was identified with that of the samples for single crystal XRD study.

Apparatus and methods

SDT 2960, simultaneous TG-DTA, TA instrument with Universal Analysis for Windows NT Ver. 2.6D was used to examine the thermal decomposition of the samples. Alumina crucibles served as reference and sample cells. All the samples were gently crushed with a pestle and mortar. The 3–5 mg of samples were subjected to a rising temperature regime over the range of ambient to 1000°C at scanning rates of 2.5, 5.0, 10.0, 15.0 and 20.0 K min^{-1} respectively. It was investigated under dry and pure nitrogen gas, which flew through the furnace chamber at a rate of 100 cm^3 min^{-1}.

The energy-dispersive spectrometer (EDS), EDAX PV9900 was employed to check the composition for both intermediates and residues.

Results and discussion

Thermal behavior

The TG-DTG and DTA curves at a heating rate of 15 K min^{-1} for both compounds studied are given in Figs 1 and 2 respectively. As seen from them, the shape of these curves is similar and both compounds show a two-step decomposition mode but with-

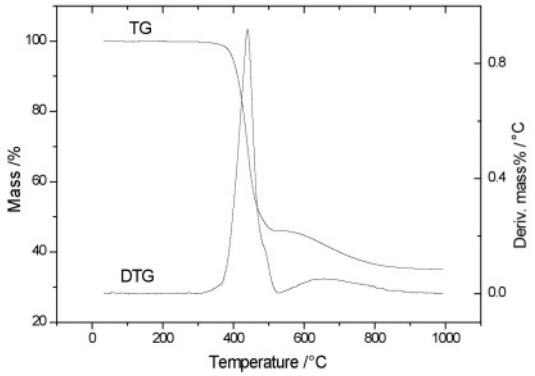

Fig. 1a TG-DTG plot of $[PPh_4]_2[C_p^*WS_3(CuBr)_3]_2$ (β=15 K min^{-1})

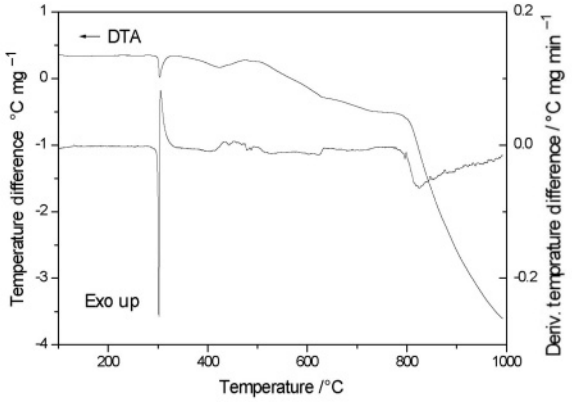

Fig. 1b DTA plot of $[PPh_4]_2[C_p^*WS_3(CuBr)_3]_2$ (β=15 K min^{-1})

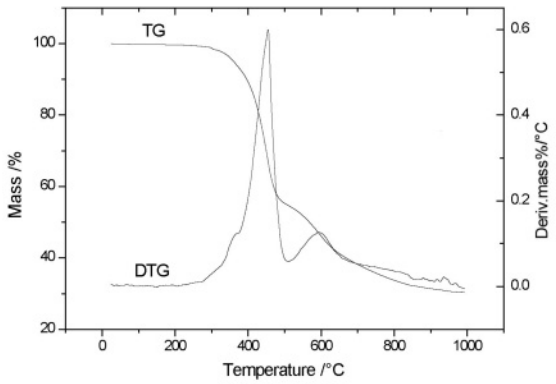

Fig. 2a TG-DTG plot of $[PPh_4]_2[C_p^*MoS_3(CuBr)_3]_2$ (β=15 K min^{-1})

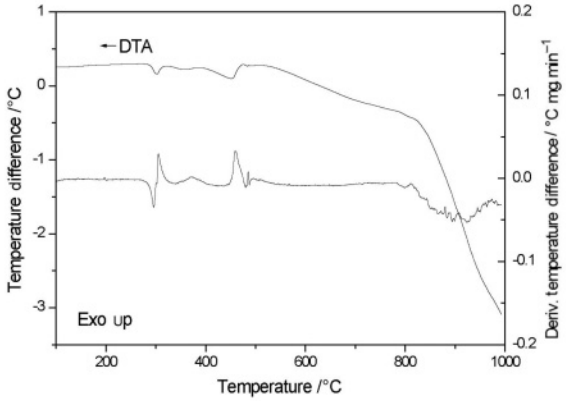

Fig. 2b DTA plot of $[PPh_4]_2[C_p^*MoS_3(CuBr)_3]_2$ (β=15 K min^{-1})

out any stable intermediate formed. As to the initial decomposition temperature, W cluster is higher than Mo cluster as the onset mass loss temperature of the first step for the former is generally higher than that for the latter at various heating rates, e.g. at β=10 K min^{-1}, it is 388°C and 333°C, respectively (Table 1).

Table 1 Thermal decomposition data for $[PPh_4]_2[C_p^*WS_3(CuBr)_3]_2$ and $[PPh_4]_2[C_p^*MoS_3(CuBr)_3]_2$ under an atmosphere of dynamic nitrogen (β=10 K min^{-1})

Compound		Temp. range/ °C	DTG peak temp. /°C	Loss of mass/%		Probable composition of expellend groups[b]
				obs.	theory	
W cluster	I.	388–495	440	0.5010	0.4813	C_p^*, PPh_4, S
	II.	495–976	603	0.1897	0.2025	Br
Mo cluster	I.	333–541	454	0.5112	0.5208	C_p^*, PPh_4, S
	II.	541–982	592	0.2087	0.2178	Br

[a]W cluster=$[PPh_4]_2[C_p^*WS_3(CuBr)_3]_2$, Mo cluster=$[PPh_4]_2[C_p^*MoS_3(CuBr)_3]_2$
[b]C_p^*=pentamethylcyclopentadienyl, PPh_4=tetraphenyl phosphorous

The mass loss percentage of the first step for either W or Mo cluster suggests that the probably expelled groups were sulfur and two organic groups, i.e. tetraphenyl phosphonium, PPh_4 and pentamethylcyclopentadienyl, C_p^*. This was confirmed by an analysis of the intermediate products of both clusters isolated immediately after the first step using the energy-dispersive spectrometer (EDS), EDAX PV9900, Fig. 3 presents this result for Mo cluster. Besides, other elemental analysis also supported this assumption, that is, after the first decomposition step, the remained composition of the intermediate product for either W or Mo cluster was W (or Mo) and CuBr. In general, it is believed in literature [11] that when competitive and independent reactions proceed concurrently in a system, the nature and details of the reaction may be

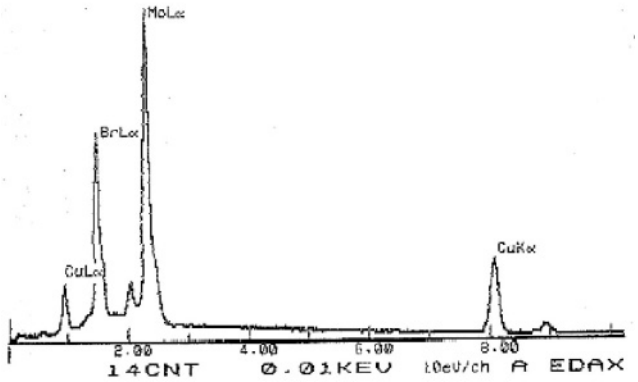

Fig. 3 EDS analysis for the intermediate of $[PPh_4]_2[C_p^*MoS_3(CuBr)_3]_2$

revealed by either increasing or decreasing the heating rates. In view of the fact that the first decomposition step for both compounds seems to include the release of more than one moiety, various heating rates were used in the present work in order to make them clearly cut from each other, but failed, even using a low heating rate 2.5 K min^{-1}, which is usually considered low enough for this purpose and thus commonly used in TA study, made no difference. Figure 4 shows this plot for Mo cluster.

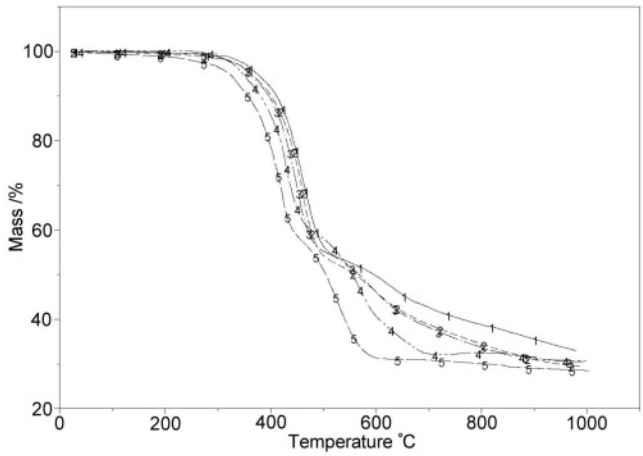

Fig. 4 Overlaid TG curve for $[PPh_4]_2[C_p^*MoS_3(CuBr)_3]_2$ using different heating rates (1 – 20, 2 – 15, 3 – 10, 4 – 5, 5 – 2.5 K min^{-1})

The mass loss and the elemental analysis using EDS indicate that the final residue at the end of decomposition was a mixture of metal W (or Mo) and Cu. Figure 5 gives the result for W cluster. The superimposed plot from various heating rates for either W or Mo (Fig. 4) cluster shows that the curve temperature shifted to higher temperature and the amount of residue increased when the heating rate increased. This result suggests the manner in which the heating rate influences the temperature distribution inside the sample. This also suggests that the various heating rates affect

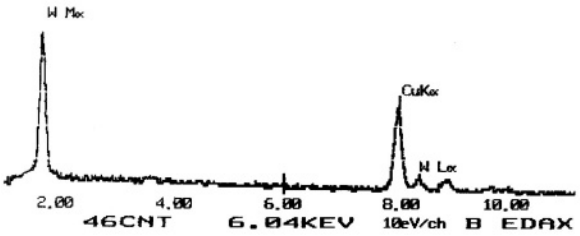

Fig. 5 EDS analysis for the residue of $[PPh_4]_2[C_p^*WS_3(CuBr)_3]_2$

the distribution of heat flux from the atmosphere to the crucible and then into sample. This is an inherent drawback of TA technique and has been widely discussed in literature [12], which could usually be somewhat reduced by trying different experimental conditions, such as using smaller sample amount and lower heating rate. As too small sample amount would lead to a greater weight error; besides, in the present study, the final residue mass is in reasonable agreement with the theoretical value (specially when $\beta \leq 10$ K min^{-1}, Table 1), the above mentioned sample mass and heating rates were employed.

It is very interesting that there is a noticeable small blip on the DTA curves at around 305°C for both clusters (Figs 1b, 2b). As it is located at the temperature which is much lower than the initial decomposition temperature, this little endothermic peak corresponds to no mass loss on TG-DTG curves. Heated to this temperature using a digital melting point apparatus, neither W nor Mo cluster gave an indication of melting. We suppose, therefore, it may be attributed to a break of the four-membered $CuBr_2Cu$ ring through which the two incomplete MS_3Cu_3 cubes of $[C_p^*MS_3Cu_3Br_3]^-$ (where *M*=W or Mo) are interconnected [9, 10] because their linkage is so weak that, in fact, the Br bridges form only in its crystalline state, not in solution [10]. Figure 6 presents a schematic drawing of W cluster dianion and selected bond distances [9], from which it can be seen that the bond length of either Cu(1)–Br(2) or Cu(2)–Br(1) is 2.876 Å i.e. 0.57 Å longer than that of Cu(1)–Br(1) or Cu(2)–Br(2).

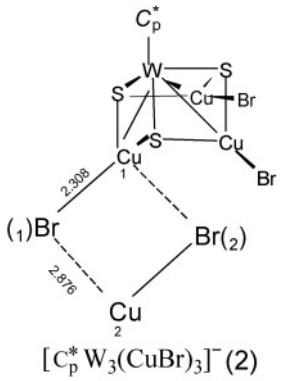

Fig. 6 Schematic drawing of $[C_p^*WS_3(CuBr)_3]_2^{1-}$

After the above-mentioned peak, a shallow broad endothermic peak can be discerned on the DTA curves roughly in the temperature region 380–500°C which corresponds to the first decomposition step for either W or Mo cluster.

Non-isothermal decomposition kinetics

The thermal analysis kinetics methods used in the present work are as follows:

Achar–Brindly–Sharp (ABS) equation [13]:

$$\ln\left[\frac{1}{f(\alpha)}\frac{\mathrm{d}\alpha}{\mathrm{d}t}\right]=\ln A-E/RT \tag{1}$$

Coats–Redfern (CR) equation [14]:

$$\ln\left[\frac{g(\alpha)}{T^2}\right]=\ln[(AE/\beta R)(1-2RT/E)]-E/RT \tag{2}$$

Kissinger equation [15]:

$$\ln\left(\frac{\beta}{T_p^2}\right)=\ln\frac{AR}{E}-E/RT_p \tag{3}$$

Flynn–Wall–Ozawa (FWO) equation [16–17]:

$$\lg\beta=\lg\left(\frac{AE}{Rg(\alpha)}\right)-2.315-0.4567E/RT \tag{4}$$

where α is the reaction fraction, $f(\alpha)$ and $g(\alpha)$ are the kinetic model function in differential and integral form respectively, E is the activation energy, A is the pre-exponential factor, β is the heating rate, R is the gas constant, T and T_p are the temperature and the peak temperature of DTG curve in K, respectively.

Table 2 The peak temperature T_p of DTG curves at various heating rates β

Compound	Stage	β/K min^{-1} (T_p/ °C)				
W cluster	I	2.5 (402)	5.0 (420)	10 (440)	15 (452)	20 (459)
	II	2.5 (550)	5.0 (583)	10 (603)	15 (611)	20 (617)
Mo cluster	I	2.5 (423)	5.0 (428)	10 (454)	15 (464)	20 (468)
	II	2.5 (532)	5.0 (577)	10 (592)	15 (598)	20 (622)

* The same as the note to Table 1

The basic data, β, T_p, obtained from TG-DTG curves are summarized in Table 2 which were used to calculate the activation energy E by both Kissinger and

Flynn–Wall–Ozawa (FWO) equations. Using the data, α, T and dα/dT from TG-DTG curves and 43 commonly used kinetic mechanism functions of $f(\alpha)$ and $g(\alpha)$ [18], the kinetic parameters E, ln$A$ and appropriate linear coefficients and standard deviation were obtained by both Achar–Brindly–Sharp (differential method) and Coats–Redfern equation (integral method) with the linear least squares method. The most probable mechanism for each decomposition stage was determined following the commonly employed method: The values of E and ln$A$ obtained by the two methods must not only be approximately equal but also corresponded to a higher linear correlation coefficient and a lower standard deviation; meanwhile, the E value calculated using both Kissinger and FWO equations were used for checking their reasonableness as multiple scanning methods are considered be able to get more reasonable activation energy E [19]. Table 3 lists the data of the first decomposition step for W and Mo cluster (β=10 K min^{-1}), respectively. (The data for the second step are omitted to save space.)

Table 3 Basic data for the first-stage decomposition reaction of both W and Mo clusters from TG-DTG curves (β=10 K min^{-1})

	$[PPh_4]_2[C_p^*WS_3(CuBr)_3]_2$			$[PPh_4]_2[C_p^*MoS_3(CuBr)_3]_2$		
No.	Temp./°C	α	dα/dT	Temp./°C	α	dα/dT
1	395.00	0.08664	0.2332	360.00	0.09505	0.1158
2	399.00	0.1083	0.2867	369.00	0.1158	0.1236
3	403.00	0.1342	0.3426	378.00	0.1375	0.1290
4	407.00	0.1650	0.4007	387.00	0.1615	0.1540
5	411.00	0.2009	0.4617	396.00	0.1909	0.1884
6	415.00	0.2416	0.5283	405.00	0.2273	0.2338
7	419.00	0.2886	0.5984	414.00	0.2727	0.2983
8	423.00	0.3412	0.6655	423.00	0.3305	0.3701
9	427.00	0.3991	0.7319	432.00	0.4009	0.4484
10	431.00	0.4629	0.8026	441.00	0.4858	0.5251
11	435.00	0.5327	0.8753	450.00	0.5814	0.5775
12	439.00	0.6081	0.9170	459.00	0.6841	0.5409
13	443.00	0.6852	0.8979	468.00	0.7583	0.3454
14	447.00	0.7575	0.8171	477.00	0.8061	0.2145
15	451.00	0.8211	0.7031	486.00	0.8353	0.1297
16	455.00	0.8745	0.5839	495.00	0.8522	0.07777
17	459.00	0.9181	0.4736	504.00	0.8635	0.06047
18	463.00	0.9530	0.3778	513.00	0.8737	0.05877
19	467.00	0.9809	0.3013	522.00	0.8840	0.06256

Table 4 The kinetic parameters of thermal decomposition for both W and Mo clusters

Compound[a]		Method[b]	E/kJ mol^{-1}	ln$A$/S^{-1}	KM[c]	r[d]	SD[e]
W cluster	I	Kissinger	134.8	7.600	AE(n=2/3)	0.9986	0.01245
		FWO	139.3	–	–	0.9999	0.005454
		ABS	129.4	9.653	AE(n=2/3)	0.9991	0.01310
		CR	128.8	10.74	AE(n=2/3)	0.9999	0.007813
	II	Kissinger	171.3	7.918	AE(n=4)	0.9804	0.1929
		FWO	176.4	–	–	0.9801	0.08412
		ABS	165.3	8.275	AE(n=4)	0.9925	0.08414
		CR	176.2	9.367	AE(n=4)	0.9988	0.08218
Mo cluster	I	Kissinger	158.7	9.213	2D	0.9825	0.2120
		FWO	162.2	–	–	0.9861	0.09204
		ABS	163.6	11.49	2D	0.9953	0.07538
		CR	156.6	11.73	2D	0.9957	0.1594
	II[f]	ABS	169.1	8.892	2D	0.9968	0.03543
		CR	176.4	9.516	2D	0.9811	0.1909

[a]The same as the notes to Table 1;
[b]FWO, Flynn–Wall–Ozawa; ABS, Achar–Brindly–Sharp; CR, Coats–Redfern method;
[c]Kinetic model; AE: Avramii–Erofeev equation;
[d]r, linear coefficient;
[e]SD standard deviation;
[f]The results for stage II of Mo cluster using both Kissinger and FWO methods were considered non-significant and discarded due to their poor linearity

Table 4 gives the complete kinetic parameters, together with their appropriate linear correlation coefficient r and standard deviation, SD, obtained from various methods for both clusters studied. It can be seen that the E and lg$A$ by the four methods are in a relatively good agreement; the first decomposition stage for W cluster was controlled by Avrami–Erofeev equation, i.e. random nucleation and nuclei growth mechanism, $f(\alpha)=(3/2)(1-\alpha)[-\ln(1-\alpha)]^{1/3}$ with the activation energy E about 130 kJ mol^{-1}; while for Mo cluster, two dimensional diffusion mechanism, $f(\alpha)=(1-\alpha)^{1/2}[1-(1-\alpha)^{1/2}]^{-1}$ with E about 160 kJ mol^{-1}. The second stage for either W or Mo cluster was governed by Avrami–Erofeev equation, $f(\alpha)=(1/4)(1-\alpha)[-\ln(1-\alpha)]^{-3}$ with E about 170 kJ mol^{-1}.

Conclusions

The thermal behavior and properties of both cluster $[PPh_4]_2[C_p^*WS_3(CuBr)_3]_2$ and $[PPh_4]_2[C_p^*MoS_3(CuBr)_3]_2$ in an atmosphere of flowing nitrogen were examined using simultaneous TG-DTA technique and discussed in connection with their distinctive molecular structure as a dianion. Supplemented using EDS method, the composition of their intermediate product was examined. Both clusters showed a two-step decom-

position mode. The first step corresponding to releasing of sulfur and two organic groups, i.e. tetraphenyl phosphonium, PPh_4 and pentamethylcyclopentadienyl, C_p^*, began at about 390°C for W cluster and 330°C for Mo cluster, respectively. Immediately after that was the second decomposition step which completed at around 800–980°C, depending on the heating rate. The final residue was metal W (or Mo) and Cu. Besides, their non-isothermal decomposition kinetics was studied using four methods. According to the experimental conditions in the present study, as sulfur concurrently releases with organic moieties, it does not seem that there exists a stable new phase composed of Mo/W–Cu–S in the decomposition process (at least when $\beta \geq 2.5$ K min^{-1}). To know whether it may exist in different conditions, e.g. isothermal condition, would need further study. In addition, since the clusters studied decompose before their melting, the CVD method may not be applicable to them.

References

1 A. Muller, E. Diemann, R. Jostes and H. Bogge, Angew. Chem., Int. Ed. Engl., 20 (1981) 934.
2 A. Muller and H. Bogger, U. Scimanski, K. Penk, K. Nieradzik, M. Dartmann, E.Krickemeyer, J. Schimanski, C. Romer, M. Romer, H. Dornfeld, U. Wienboker and W. Hellmann, Monatsh. Chem., 120 (1989) 367.
3 Y. Jeannin, F. Secheresse, S. Bernes and F. Roberd, Inorg. Chim. Acta, 198–200 (1992) 493.
4 W. Eltzner, M. Breysse, M. Lacroix and M. Vriant, Polyhedron, 5 (1986) 203.
5 R . H. Holm, Pure Appl. Chem., 67 (1995) 2117.
6 R. Chevrel, M. Hirrien and M. Sergent, Polyhedron, 5 (1986) 87.
7 J. Lang, Q. Xu and S. Ji, Chinese Journal of Inorganic Chemistry (in Chinese), 17 (2001) 609.
8 S. Shi and W. Ji, S. Tang, J. Lang and Q. Xin, J. Am. Chem. Soc., 116 (1994) 3615.
9 J. Lang, H. Kawaguchi, S. Ohnishi and K. Tatsumi, Chem. Commun., (1997) 405.
10 J. Lang, H. Kawaguchi, S. Ohnishi and K. Tatsumi, Inorg. Chim. Acta, 283 (1998) 136.
11 A. Ortega, Thermochim. Acta, 284 (1996) 379.
12 Y. Huang, Y. Cheng, K. Alexander and D. Dollimore, Thermochim. Acta, 367–368 (2001) 43.
13 B. N. Achar, G. W. Brindley and J. H. Sharp, Proc. Int. Clay Conf. Jerusalem, 1 (1966) 67.
14 A. W. Coats and J. P. Redfern, Nature, 201 (1964) 68.
15 H. E. Kissinger, Anal. Chem., 29 (1957) 1702.
16 T. Ozawa, Bull. Chem. Soc. Jpn., 38 (1965) 1881.
17 J. H. Flynn and L. A. Wall, J. Polym. Sci. Part B, Polymer Letters, 4 (1966) 323.
18 R. Hu and Q. Shi, Thermal Analysis Kinetics (in Chinese), Science Press, Beijing 2001, p. 127.
19 Z. Lu, Chinese Journal of Inorganic Chemistry (in Chinese), 14 (1998) 119.